Molecular Dynamics of Benzene in Neat Liquid and a Solution Containing Polystyrene. ^{13}C Nuclear Magnetic Relaxation and Molecular Dynamics Simulation Results

Richard Witt, Laszlo Sturz, and Andreas Dölle*

Institut für Physikalische Chemie, Rheinisch-Westfälische Technische Hochschule, D-52056 Aachen, Germany

Florian Müller-Plathe

Max-Planck-Institut für Polymerforschung, D-55128 Mainz, Germany

Received: January 14, 2000

The reorientational motion of benzene in the neat liquid and in a polystyrene/benzene solution was investigated by NMR relaxation as well as MD simulation methods. The temperature-dependent ^{13}C dipolar spin−lattice relaxation rates and cross correlation rates between the dipolar relaxation mechanism and the relaxation by chemical-shift anisotropy were measured. From the NMR measurements and MD simulation results, the rotational diffusion constants for rotations about the C_6 axis and perpendicular to it were evaluated, and it was found that the values of the former were larger than those of the latter. The rotational anisotropy, which is the ratio of these values, decreases for the NMR data from 2.3 to 1.2 when increasing the temperature from 280 to 323 K. The activation energy for reorientation about the main symmetry axis was 3.4 kJ mol^{-1} and about axes perpendicular to that 13.3 kJ mol^{-1}. The temperature effect was less pronounced for the MD results; the anisotropy changed from 1.9 to 1.3 between 280 and 360 K. The reorientational correlation functions showed a significant non-Debye behavior and were fitted with a Kohlrausch-Williams-Watts function. Furthermore, from the MD simulations the temperature dependence of the density and the translational diffusion coefficient were also determined. The NMR data for benzene rotational motions in a polystyrene matrix could not be explained by a simple rotational diffusion model. From the data, it was concluded that the rotations about the C_6 axis were much faster than about axes perpendicular to the C_6 axis. This finding is in accordance to a previous MD study by Müller-Plathe.

Introduction

Benzene is of great importance as a solvent in technical and industrial use. Furthermore, it is often used as a model compound to study structure and dynamics in liquids. However, it was for a long time difficult to obtain reliable experimental data on the anisotropy of the molecular reorientational motion. In Table 1, all data found by the authors in the literature[1−18] are listed, showing that values between 0.56 and 6.7 were obtained for the anisotropy. In the studies before 1980, a major difficulty was that often different methods had to be applied for the different components of reorientational motion because of methodological problems. This caused doubts about the reliability of the obtained results.

From conventional NMR relaxation experiments alone, that is, relaxation via the dipolar or quadrupolar pathway, only the reorientation of vectors in the molecular plane (in-plane reorientation, index i) could be observed because of the symmetry of the benzene molecule. In a previous paper[11] in 1991 Dölle et al. reported on the anisotropy of the reorientational dynamics, which was the first study using exclusively NMR data for evaluating the anisotropy. In this study, the in-plane reorientational correlation time τ_{2i} (for a definition see below) was obtained from the dipolar (DD) ^{13}C spin-lattice relaxation time of [$^1H_6$]benzene, and $R_\perp$ was obtained from the chemical-shift anisotropy (CSA) contribution to the ^{13}C spin−lattice relaxation of [$^2H_6$]benzene. $R_\perp$ is the rotational diffusion constant for rotations about an axis perpendicular to the C_6 axis of the benzene molecule, whereas $R_\parallel$ is the rotational diffusion constant for rotations parallel to the C_6 axis. In the following, studies by Coupry et al.[12] and Python et al.[17] were published in which ^{13}C dipolar spin−lattice relaxation rates were combined with measurements of the ^{13}C DD−CSA cross correlation rates to yield the desired data. However, the observed anisotropies still differ among the more recent studies by almost 100%. A possible source of the disagreement could be the differing temperatures at which these studies were performed.

Polymer/solvent systems are taken as model systems for solvent motion in restricted geometries. Because of the interaction of the solvent molecules with the surrounding polymer matrix, conclusions concerning the dynamics of the polymer itself can also be drawn. Müller-Plathe[14,15] studied the dynamics of the solvent benzene in neat liquid and in polystyrene swollen in benzene by molecular dynamics (MD) simulations. The reorientational motion about the C_6 axis was faster than that perpendicular to that axis. For the neat liquid, the ratio of $1/(6\tau_i)$ to $R_\perp$ was found to be 1.6, and it increased drastically by 2 to 3 orders of magnitude with increasing polymer concentrations. Meanwhile, similar enhancements of the reorientational anisotropy with polymer content were also found for water molecules in mixtures with poly(vinyl alcohol) investigated by MD simulations.[16]

It was the aim of the present study to perform experiments with high accuracy only on nondeuterated benzene to avoid any

* Author to whom correspondence should be addressed. E-mail: doelle@rwth-aachen.de.

10.1021/jp000201p CCC: $19.00
Published on Web 06/15/2000

TABLE 1: Compilation of Experimental Results for the Anisotropy of the Molecular Reorientational Dynamics of Benzene in Neat Liquid

T/K	$(1/(6\tau_i))/10^{10}$ s^{-1}	$R_\perp/10^{10}$ s^{-1}	$R_\parallel/10^{10}$ s^{-1}	$\sigma = R_\parallel/R_\perp$	method	authors
303		13	14	1.1	^{2}H T_1 (indirect)	W. T. Huntress (1969)
296		6.3	5.2	0.8	Raman	F. J. Bartoli and T. A. Litovitz (1972)
298		5.4	36	6.7	^{2}H T_1/Raman	K. T. Gillen and J. E. Griffiths (1972)
296	11	5.7	21	2.4	depolarized RS/^{13}C T_1	D. R. Bauer et al. (1974)
303	11.7	8.0	18.7	2.3	^{2}H T_1/Raman (50 bar)	K. Tanabe and J. Jonas (1977)
302		16	8.9	0.56	^{2}H and ^{13}C T_1	O. Yamamoto and M. Yanagisawa (1978)
		8.9	18	2.0	IR/Raman	K. Tanabe (1979)
		9.1	22	2.4	Raman	K. Tanabe and J. Hiraishi (1980)
288	12.8	7.2	22	3.1	MD ($\rho = 0.92\ \rho_{exp}$)	O. Steinhauser (1982)
312		14	27	1.9	MD	P. Linse et al. (1985)
293	12.7	10.2	15.9	1.6	^{13}C T_1	A. Dölle et al. (1991)
283		8.0	19.2	2.4	^{13}C T_1	C. Coupry et al. (1994)
295		8.7	24.8	2.9	Raman	J. Yi and J. Jonas (1996)
300	16.4	10.1	26.0	2.6	MD	F. Müller-Plathe (1996)
298	17.7	10.3	28.8	2.8	^{13}C T_1	H. Python et al. (1997)
293	12.6	7.41	21.1	2.8	Raman (Tanabe)/^{2}H T_1	A. Laaksonen et al. (1998)
298		9.52	14.4	1.4	MD	A. Laaksonen et al. (1998)

influences from dynamic isotope effects. From these experiments, the anisotropy of rotational motion was obtained. Furthermore, temperature-dependent measurements were performed, and the activation parameters for the anisotropic molecular rotational motion of benzene in the neat liquid were evaluated. To the knowledge of the authors, the determination of these parameters solely by NMR experiments was achieved in the present investigation for the first time. The NMR results are compared to new MD simulation results in this study. Determination of the rotational dynamics in a solution of polystyrene in benzene demonstrates the effects of restricted geometries on reorientational dynamics.

Theoretical Background

Translational and Reorientational Molecular Dynamics. Transport coefficients γ are given by infinite time integrals of an equilibrium time correlation function $C(\tau) = \langle \dot{A}(\tau)\dot{A}(0)\rangle$ for the time derivative of the arbitrary quantity A:[19,20]

$$\gamma = \int_0^\infty \langle \dot{A}(t)\dot{A}(0)\rangle \, dt \tag{1}$$

which is related for large times to an "Einstein expression" by

$$2t\gamma = \langle (A(t) - A(0))^2 \rangle \tag{2}$$

Translational diffusional motion of molecules in isotropic liquids are thus described by the (self-) diffusion constant D:

$$D = \frac{1}{3}\int_0^\infty \langle \boldsymbol{v}(t)\boldsymbol{v}(0)\rangle \, dt \tag{3}$$

with the velocity $\boldsymbol{v}$ as the time derivative of the space coordinates. The diffusion constant is, according to eq 2, related to the mean square displacements by

$$6Dt = \langle |\boldsymbol{r}(t) - \boldsymbol{r}(0)|^2 \rangle \tag{4}$$

Analogous expressions are obtained for the rotational diffusion constants R_i about the rotational diffusion principal axis i with the angular velocity ω_i:[21,22]

$$R_i = \int_0^\infty \langle \omega_i(t)\omega_i(0)\rangle \, dt \tag{5}$$

and[22,23]

$$2R_i t = \langle |\theta_i(t) - \theta_i(0)|^2 \rangle \tag{6}$$

where $\theta_i(t)$ and $\theta_i(0)$ are the orientations at time t and $t = 0$, respectively, and θ_i is a nonperiodic, unbounded quantity representing the angle of reorientation about the principal axis i.

Another approach to describe reorientational motions of rigid molecules is to evaluate the probability density $p(\delta\boldsymbol{\Omega},t)$ that a molecule reorients by $\delta\boldsymbol{\Omega}$, where $\boldsymbol{\Omega}$ is given by the set of Eulerian angles (α, β, γ), from orientation $\boldsymbol{\Omega}_0$ at time $t = 0$ to orientation $\boldsymbol{\Omega}$ at time t.[21,22,24−27] The probability density is expanded in a complete set of the Wigner matrix elements $D^l_{mm'}(\Omega,t)$:[26]

$$p(\delta\boldsymbol{\Omega},t) = \frac{1}{8\pi^2}\sum_{k,k',l}(2l+1)\, C^l_{kk'}(t) D^{l*}_{kk'}(\delta\boldsymbol{\Omega},t) \tag{7}$$

where the expansion coefficients

$$C^l_{kk'} = (2l+1)\langle D^l_{nk}(\boldsymbol{\Omega},t) D^{l*}_{nk'}(\boldsymbol{\Omega}_0,0)\rangle = \langle D^l_{kk'}(\delta\boldsymbol{\Omega},t)\rangle \tag{8}$$

are the orientational time correlation functions.[20,26−29] In the case of "small−step" reorientations, a diffusion equation is formulated:[21,22,24,25,27,30]

$$\frac{\partial p(\delta\boldsymbol{\Omega},t)}{\partial t} = -(\hat{\boldsymbol{L}}\mathbf{R}\hat{\boldsymbol{L}})p(\delta\boldsymbol{\Omega},t) \tag{9}$$

in which $\hat{\mathbf{L}}$ is the quantum−mechanical angular momentum operator and $\mathbf{R}$ the rotational diffusion tensor, which is symmetric in isotropic liquids.[27] The rotational diffusion constants are given by the diagonal elements R_{ii} of the rotational diffusion tensor in its principal axis system and defined according to eq 6.[22,27] As a result of the symmetry of the benzene molecule, the orientation of the rotational diffusion principal axis system is identical with the orientation of the inertial prinicpal axis system.[31] Equation 9 is of the same form as the Schrödinger equation for the rigid rotator, and, therefore, the solutions of the latter can be used for solving eq 9.

For the case of isotropic liquids, and after normalization, a reduced correlation function $C^l_m(t)$ is obtained with $m = k = k'$. Its time integral is defined as the correlation time τ_{lm}:

$$\tau_{lm} = \int_0^\infty C^l_m(t)\, dt \tag{10}$$

When the reorientational motions are of stochastic, that is, diffusive nature, and when only one ensemble of reorienting units is present, the correlation functions are given by an

exponential function:[32]

$$C_m^l(t) = \exp(-t/\tau_{lm}) \tag{11}$$

One criterion, whether the model of "small−step" rotational diffusion is valid for the investigated rotational motion or whether inertial effects are predominating, is the χ test introduced by Wallach and Huntress.[33] If the reorientational correlation time $(\tau_\theta)_i$ about the ith rotation axis is essentially larger than the mean period $(\tau_f)_i$ of free rotation about the corresponding axis, the molecular rotational motion is in the region of rotational diffusion, and the following relation is valid:

$$(\chi)_i = \left(\frac{\tau_\theta}{\tau_f}\right)_i = \frac{5}{18R_i}\left(\frac{kT}{I_i}\right)^{1/2} \gg 1 \tag{12}$$

The classification by Gillen and Noggle[34] can be used as a limiting criterion:

$$(\chi)_i < 3 \text{ inertial regime}$$

$$3 < (\chi)_i < 5 \text{ intermediate regime}$$

$$5 < (\chi)_i \text{ rotational diffusion regime}$$

Furthermore, from theoretical considerations as well as from the experimental data it becomes obvious that the assumption of an exponential decay for the correlation function is only an approximation. To fit better to the experimental data, often empirical forms are used for the correlation functions. One of these is the stretched exponential or Kohlrausch−Williams−Watts function[35,36]

$$C_{m,\mathrm{KWW}}^l = \exp[(-t/\alpha_m^l)^{\beta_m^l}] \tag{13}$$

for which the time integral is analytical[37]

$$\tau_{lm,\mathrm{KWW}} = \int_0^\infty C_{m,\mathrm{KWW}}^l(t)\,\mathrm{d}t = \frac{\alpha_m^l}{\beta_m^l}\Gamma\left(\frac{1}{\beta_m^l}\right) \tag{14}$$

with the gamma function $\Gamma(x)$.

Rotational diffusion is a thermally activated process and thus, even for correlation functions deviating from the simple exponential behavior of the rotational diffusion case, an Arrhenius equation is often valid in describing the temperature dependence of either the correlation times

$$\tau_i = \tau_{0i}\exp(E_{\mathrm{A}i}/RT) \tag{15}$$

or of the rotational diffusion constants

$$R_i = R_{0i}\exp(-E_{\mathrm{A}i}/RT) \tag{16}$$

The $E_{\mathrm{A}i}$ are the corresponding activation energies.

The reorientation of a molecule−fixed unit vector $\boldsymbol{u}$ is described by the time correlation functions of the matrix elements $D_{00}^l(\Omega,t)$:

$$C_0^l(t) = \langle D_{00}^l(\delta\boldsymbol{\Omega},t)\rangle = \langle P_l[\cos(\beta(t))]\rangle \tag{17}$$

where the $P_l[\cos(\beta(t))]$ are the Legendre polynomials. Infrared linewidths or dielectric relaxation probe the case $l = 1$:

$$C_0^1(t) = \langle P_1[\cos(\beta(t))]\rangle = \langle \boldsymbol{u}(t)\boldsymbol{u}(0)\rangle \tag{18}$$

whereas for Raman and NMR relaxation, $l = 2$:

$$C_0^2(t) = \langle P_2[\cos(\beta(t))]\rangle = \left\langle \frac{1}{2}[3(\boldsymbol{u}(t)\boldsymbol{u}(0))^2 - 1]\right\rangle \tag{19}$$

The observed NMR relaxation rates are related to the molecular dynamics by reduced spectral densities that are obtained from the reduced correlation functions by Fourier transformation:

$$J_{lm}(\omega_\lambda,\{x_i\}) = \int_{-\infty}^{\infty} C_m^l(t,\{x_i\})\exp(\mathrm{i}\omega_\lambda t)\,\mathrm{d}t \tag{20}$$

where ω_λ is the transition frequency and $\{x_i\}$ are the characteristic parameters in the correlation functions. The result of the Fourier transformation for the case of the exponential correlation function is

$$J_{lm}(\omega_\lambda) = \frac{2\tau_{lm,\mathrm{BPP}}}{1 + (\omega_\lambda\tau_{lm,\mathrm{BPP}})^2} \tag{21}$$

which corresponds to a Lorentzian function and which was used for the first time by Bloembergen, Purcell, and Pound[38] for the interpretation of NMR relaxation data. The parameter $\tau_{lm,\mathrm{BPP}}$ is the correlation time for rotational diffusion, that is, for an exponential correlation function. When the extreme narrowing condition, that is, the condition $\omega_\lambda\tau_{lm} \ll 1$, is valid, the BPP spectral density reduces to

$$J_{lm\lambda,\mathrm{BPP}} = 2\tau_{lm,\mathrm{BPP}} \tag{22}$$

Longitudinal Relaxation in the ^{13}C−^{1}H Spin System. The relaxation in ^{13}C−^{1}H spin systems can be described with the formalism by Grant et al.[27] or Canet.[39] The longitudinal relaxation is given by the time dependence of the so-called magnetization modes:

$$\frac{\mathrm{d}\boldsymbol{\nu}(t)}{\mathrm{d}t} = -\boldsymbol{\Gamma}\boldsymbol{\nu}(t) \tag{23}$$

in which $\boldsymbol{\Gamma}$ is the relaxation matrix and the vector $\boldsymbol{\nu}(t)$ contains the magnetization modes. The latter are given by the relations

$$\boldsymbol{\nu}_1(t) = \langle \boldsymbol{I}_{\mathrm{C}z}\rangle - \boldsymbol{I}_{\mathrm{C}}^{\mathrm{eq}}$$

$$\boldsymbol{\nu}_2(t) = \langle \boldsymbol{I}_{\mathrm{H}z}\rangle - \boldsymbol{I}_{\mathrm{H}}^{\mathrm{eq}}$$

$$\boldsymbol{\nu}_3(t) = 2\langle \boldsymbol{I}_{\mathrm{C}z}\boldsymbol{I}_{\mathrm{H}z}\rangle$$

$$\boldsymbol{\nu}_4(t) = \boldsymbol{E}/2 \tag{24}$$

in which the magnetization modes $\boldsymbol{\nu}_1$ and $\boldsymbol{\nu}_2$ correspond to the total ^{13}C and ^{1}H polarization after subtraction of the corresponding values for thermal equilibrium $\boldsymbol{I}_{\mathrm{C}}^{\mathrm{eq}}$ and $\boldsymbol{I}_{\mathrm{H}}^{\mathrm{eq}}$, $\boldsymbol{\nu}_3$ to the longitudinal two-spin order of spins ^{13}C and ^{1}H, and $\boldsymbol{\nu}_4$ to the sum over the populations of the energy levels for the spin system ^{13}C−^{1}H. $\langle \boldsymbol{I}_{\mathrm{C}z}\rangle$ and $\langle \boldsymbol{I}_{\mathrm{H}z}\rangle$ are the expectation values for the z components of the ^{13}C and ^{1}H spin operators, respectively, and $\boldsymbol{E}$ is the identity operator.

The relaxation matrix is symmetric ($\Gamma_{ij} = \Gamma_{ji}$), and its matrix elements are linear combinations of the spectral densities. The elements Γ_{23}, Γ_{32}, are negligible because of the small chemical-shift anisotropy for protons, whereas Γ_{4n} and Γ_{m4} vanish. Following the notation by Grant et al.[27] and when the extreme narrowing condition is valid, the remaining elements for benzene are (the index l in the spectral densities being equal to 2 is omitted in the following)

$$\Gamma_{11} = \frac{1}{T_1^{DD}} + \frac{1}{T_1^{CSA}} + ... = \frac{1}{12} J^{DD} + J^{CSA} + ... \quad (25)$$

where

$$J^{DD} = \frac{3}{2}\sum_{i=1}^{n_H} (2\pi D_i)^2 (J_{20} + 3J_{22}) = 3\sum_{i=1}^{n_H} (2\pi D_i)^2 (\tau_{20} + 3\tau_{22}) \quad (26)$$

is the spectral density for the $n_H = 6$ dipolar interactions between the ^{13}C nucleus and the protons in the benzene molecule. The dipolar coupling constant is related to the distance r_i between the ^{13}C nucleus and proton i by

$$D_i = \frac{\mu_0}{8\pi^2} \gamma_C \gamma_H \hbar r_i^{-3} \quad (27)$$

with the magnetogyric ratios for ^{13}C and ^{1}H of γ_C and γ_H, respectively, the magnetic permeability μ_0, and the Planck constant $\hbar = h/2\pi$. The correlation times τ_{2m} and the rotational diffusion constants for the symmetric diffusor benzene are connected by

$$\tau_{2m} = \frac{1}{6R_\perp + m^2(R_\parallel - R_\perp)} \quad (28)$$

and thus for the dipolar spectral density

$$J^{DD} = \sum_{i=1}^{n_H} (2\pi D_i)^2 \frac{5R_\perp + R_\parallel}{R_\perp(R_\perp + 2R_\parallel)} = 12\sum_{i=1}^{n_H} (2\pi D_i)^2 \tau_{2i} \quad (29)$$

$R_\parallel$ and $R_\perp$ are the rotational diffusion constants about the C_6 axis and perpendicular to that axis. The reorientation of the $^{13}C-^{1}H$ vector in the aromatic plane is described by the in-plane correlation time:

$$\tau_{2i} = \frac{1}{4}(\tau_{20} + 3\tau_{22}) \quad (30)$$

From eqs 28 and 30, it follows that for planar molecules that are symmetric rotators

$$\tau_{2i} = \frac{1}{24R_\perp} + \frac{3}{4}\frac{1}{2R_\perp + 4R_\parallel} \quad (31)$$

The spectral density for the interaction by chemical-shift anisotropy is

$$J^{CSA} = \frac{1}{15}\gamma_C^2 B_0^2 (\Delta\sigma)^2 \left(J_{20} + \frac{\eta^2}{3} J_{22}\right) = \frac{2}{15}\gamma_C^2 B_0^2 (\Delta\sigma)^2 \left(\tau_{20} + \frac{\eta^2}{3}\tau_{22}\right) \quad (32)$$

with the ^{13}C shielding anisotropy

$$\Delta\sigma = \sigma_{ZZ} - \frac{\sigma_{XX} + \sigma_{YY}}{2} \quad (22)$$

and the asymmetry factor

$$\eta = \frac{3(\sigma_{XX} - \sigma_{YY})}{2\Delta\sigma} \quad (34)$$

where σ_{XX}, σ_{YY}, and σ_{ZZ} are the diagonal elements of the shielding tensor in its principal axis frame with $|\sigma_{ZZ}| \geq |\sigma_{YY}| \geq |\sigma_{XX}|$, and B_0 is the magnetic flux density of the external magnetic field. From eq 28,

$$J^{CSA} = \frac{1}{45}\gamma_C^2 B_0^2 (\Delta\sigma)^2 \left(\frac{1}{R_\perp} + \eta^2 \frac{1}{R_\perp + 2R_\parallel}\right) \quad (35)$$

Often a so-called leakage term j represents further spectral densities resulting from other relaxation pathways. For the experimental conditions chosen in the present study, it is equal to the contribution from the spin rotation mechanism SR, and thus

$$\Gamma_{11} = \frac{1}{T_1^{DD}} + \frac{1}{T_1^{CSA}} + \frac{1}{T_1^{SR}} \quad (36)$$

Whereas Γ_{11} corresponds to the total longitudinal relaxation rate $1/T_1$ of the ^{13}C nuclei, $\Gamma_{12} = \sigma = (5/12)J^{DD}$ is the cross relaxation rate. The latter is related to the nuclear Overhauser (NOE) factor η_{C-H} for relaxation by n_H protons i by[40]

$$\eta_{C-H} = \frac{\gamma_H}{\gamma_C} \frac{\sum_{i=1}^{n_H} \sigma_i}{\sum_{i=1}^{n_H} \rho_i + \rho^*} \quad (37)$$

where $\rho_i = (1/T_1^{DD})_i$ is the dipolar relaxation rate resulting from proton i and ρ^* is the leakage term corresponding to the spectral density j, which reduces the NOE factor. The term $1/T_1^{DD-CSA} = -\Gamma_{13} = -(1/2)J^{DD-CSA}$ can be called the ^{13}C cross correlation relaxation rate resulting from dipolar and chemical-shift anisotropy mechanisms with the spectral density

$$J^{DD-CSA} = -\frac{1}{5} D(\Delta\sigma)\gamma_C B_0 (J_{20} + \eta J_{22}) = -\frac{2}{5} D(\Delta\sigma)\gamma_C B_0 (\tau_{20} + \eta\tau_{22}) \quad (38)$$

or

$$J^{DD-CSA} = -\frac{1}{5} D(\Delta\sigma)\gamma_C B_0 \left(\frac{1}{3R_\perp} + \eta\frac{1}{R_\perp + 2R_\parallel}\right) \quad (39)$$

respectively.

The remaining matrix elements are not of interest for the present study and will therefore not be discussed further.

Results

Molecular Dynamics Simulations of Neat Benzene. The MD simulations yielded data for the mass density ρ, the translational diffusion coefficient D, the rotational correlation times $\tau_{l\parallel}$ and $\tau_{l\perp}$, and the corresponding Kohlrausch exponents $\beta_{l\parallel}$ and $\beta_{l\perp}$ in the temperature range 240 to 360 K. The results are given in Table 2. The temperature dependence of the mass density appears to be linear with temperature and is shown in Figure 1 together with the fit function of experimental values by Klüner.[41] The MD results for the dependence of the diffusion coefficients on $1/T$ is given in Figure 2 with an experimental fit function obtained by Ertl and Dullien.[42]

^{13}C NMR Relaxation Data for Neat Benzene. The total longitudinal spin−lattice relaxation rates $1/T_1$, the NOE factors η_{C-H}, and the DD−CSA cross correlation relaxation rates $1/T_1^{DD-CSA}$ were measured in a temperature range from 280 to 323 K at a ^{13}C resonance frequency of 62.89 MHz. These values

TABLE 2: Temperature Dependence of the Data Obtained from MD Simulations for Neat Benzene (Density ρ, Diffusion Coefficient D, Correlation Times τ_{li} and $\tau_{l\perp}$, and Coefficients β_{li} and $\beta_{l\perp}$ for Reorientation of a Vector in the Molecular plane and Perpendicular to It)

T/K	t/ps[a]	ρ/kg/m^{-3} [b]	D/10^{-9} m^2 s^{-1} [c]	τ_{1i}/ps β_{1i}	$\tau_{1\perp}$/ps $\beta_{1\perp}$	τ_{2i}/ps β_{2i}	$\tau_{2\perp}$/ps $\beta_{2\perp}$
240	1163	945 (4.5)	0.22 (0.011)	6.3	15	2.9	5.9
				0.92	0.80	0.70	0.58
260	270	917 (4.8)	0.59 (0.059)	4.5	9.1	1.8	2.9
				0.91	0.81	0.77	0.67
280	158	893 (2.5)	1.1 (0.12)	3.3	5.5	1.3	1.9
				0.94	0.87	0.85	0.73
300	238	872 (6.7)	1.4 (0.12)	2.8	4.5	1.2	1.5
				0.98	0.89	0.87	0.77
320	468	845 (6.1)	2.3 (0.13)	2.3	3.4	0.93	1.2
				1.0	0.90	0.93	0.82
340	187	823 (3.9)	2.9 (0.12)	1.0	2.9	0.81	0.96
				1.0	0.91	0.97	0.87
360	110	795 (4.6)	4.3 (0.69)	1.7	2.3	0.68	0.77
				1.0	0.96	1.0	0.93

[a] Total simulation time. [b] Fluctuation in parentheses. [c] Error in parentheses.

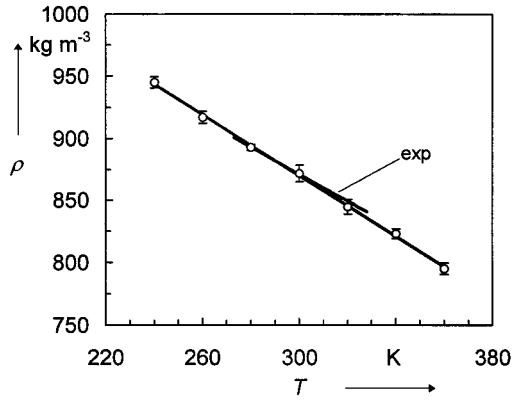

Figure 1. Mass density ρ. Data points were obtained from MD simulations, and lines were calculated from the parameters as well as from a fit to experimental data points.

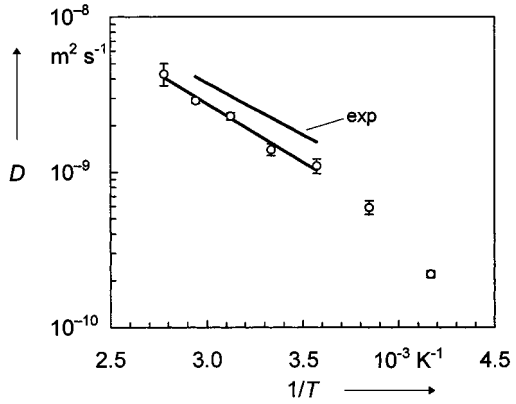

Figure 2. Translational diffusion coefficient D. Data points were obtained from MD simulations, and lines were calculated from an Arrhenius fit to the MD simulation results as well as to experimental data points.

and the dipolar longitudinal relaxation rates $1/T_1^{DD}$ are contained in Table 3 together with the results from measurements at 75.47 and 100.62 MHz and from ref 11 at 22.63 MHz for a temperature of 293 K. The results for the different relaxation rates at 62.89 MHz are plotted in Figure 3 as a function of the reciprocal temperature, whereas in Figure 4, the total relaxation rates at 293 K are shown as a function of the square of the magnetic flux density.

TABLE 3: Temperature and Frequency Dependence of the Total Longitudinal ^{13}C Relaxation Rates $1/T_1$, Nuclear Overhauser Factors η_{C-H}, Dipolar Longitudinal Relaxation Rates $1/T_1^{DD}$, and DD−CSA Cross Correlation Relaxation Rates $1/T_1^{DD-CSA}$ for Benzene in Neat Liquid

T/K	ν(^{13}C)/MHz	$1/T_1$/10^{-2} s^{-1}	η_{C-H}	$1/T_1^{DD}$/ 10^{-2} s^{-1}	$1/T_1^{DD-CSA}$/ 10^{-2} s^{-1}
280	62.89	4.07	1.58	3.24	0.685
281		4.02	1.58	3.20	0.680
283		3.90	1.59	3.13	0.650
285		3.85	1.56	3.03	0.630
288		3.80	1.57	3.00	0.610
293		3.74	1.46	2.75	0.550
298		3.61	1.45	2.63	0.505
303		3.45	1.39	2.42	0.470
308		3.38	1.38	2.34	0.446
313		3.29	1.36	2.25	0.425
318		3.26	1.32	2.16	0.394
323		3.20	1.26	2.02	0.356
293	22.63[a]	3.45	1.61	2.79	
	75.47	3.69	1.46	2.71	
	100.62	3.88	1.48	2.89	

[a] Data from ref 11.

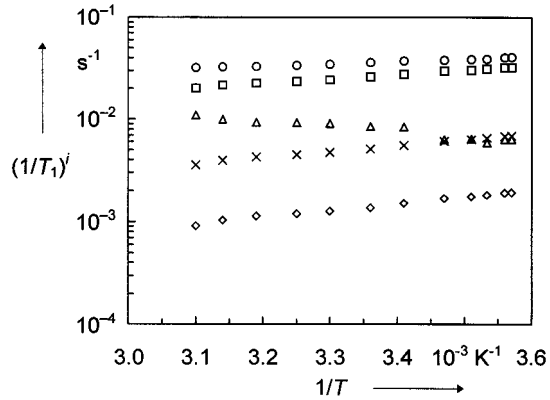

Figure 3. ^{13}C longitudinal relaxation rates at 62.89 MHz as a function of reciprocal temperature: total (○), dipolar (□), spin rotation (△), chemical-shift anisotropy (◇), and cross correlation DD-CSA (×).

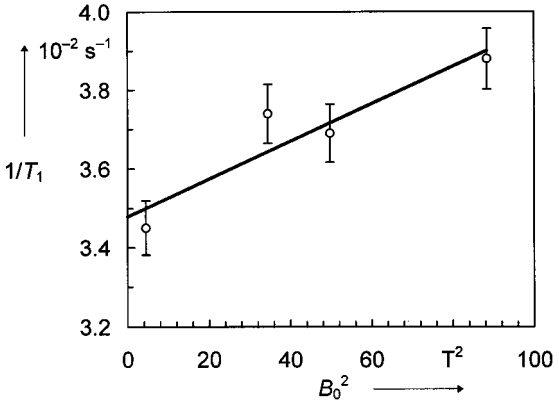

Figure 4. Total ^{13}C longitudinal relaxation rates $1/T_1$ at 293 K as a function of the square of the magnetic flux density B_0. The error bars correspond to an error of 2%.

Rotational Molecular Dynamics of Neat Benzene. The reorientational correlation functions $C_0^l(t)$ with $l = 1, 2$ for vectors in the aromatic plane and perpendicular to it that were obtained from MD simulations are shown in Figure 5 for a temperature of 300 K as an example. The dependence of the correlation times τ_{li} and $\tau_{l\perp}$ on $1/T$ is presented in Figure 6. After fitting of an Arrhenius relation according to eq 15 to the data points between 280 and 360 K, the activation energies in Table 4 were obtained.

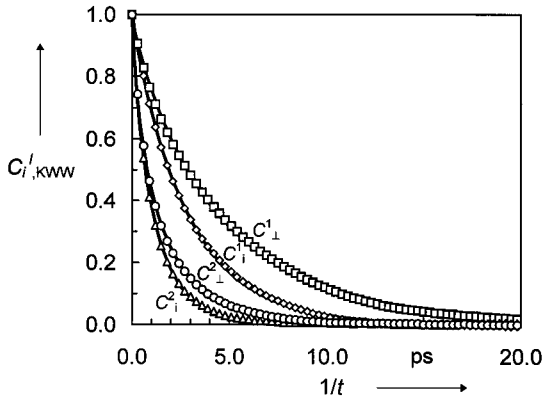

Figure 5. Reorientational correlation functions of vectors in and perpendicular to the aromatic plane, $C^l_{i,KWW}$ and $C^l_{\perp,KWW}$, respectively. Lines were obtained from a fit of eq 13 to MD simulation results at 300 K.

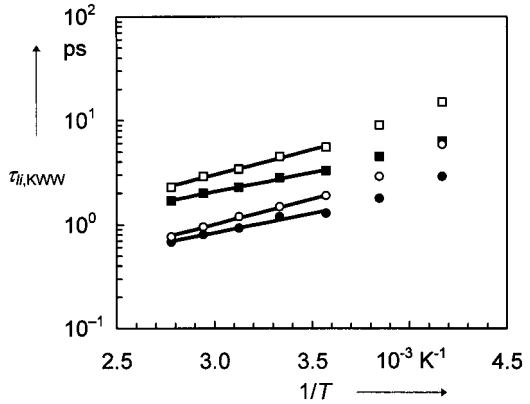

Figure 6. Reorientational correlation times of vectors in and perpendicular to the aromatic plane, $\tau_{li,KWW}$ and $\tau_{l\perp,KWW}$, respectively. Lines were obtained from an Arrhenius fit to the MD simulation results.

TABLE 4: Activation Parameters for Molecular Reorientational Motion of Neat Benzene: Activation Energies E_{Ai} (kJ mol^{-1}), and Preexponential Factors R_{0i} (10^{12} rad^2 s^{-1})

	MD	NMR
E_{A1i}	7.1 ± 0.4	
$E_{A1\perp}$	9.2 ± 0.5	
E_{A2i}	7.0 ± 0.4	8.2 ± 0.3
$E_{A2\perp}$	9.3 ± 0.4	13.3 ± 0.3
$E_{A2\|\|}$		3.4 ± 0.3
R_{0i}		3.7 ± 0.4
$R_{0\perp}$		1.9 ± 0.2
$R_{0\|\|}$		0.77 ± 0.09

In Figure 7, the results for $1/(6\tau_{2i})$ and the rotational diffusion constants $R_\perp$ and $R_\|$ evaluated from the MD simulations are compared to the corresponding values from the NMR relaxation data. The former were obtained from the reorientational correlation times calculated from the fit functions with $R_\perp = 1/(6\tau_{2\perp})$ and with the help of eq 28. The Arrhenius function in eq 16 was fitted to the rotational diffusion constants from the NMR data. These activation energies and also the preexponential factors are given in Table 4.

Solution of Polystyrene in Benzene. At a temperature of 300 K, the corresponding relaxation rates of benzene were measured in a solution of 56% polystyrene (Polystyrene Standard 10 000 by Fluka, Switzerland) corresponding to a mole fraction of $x = 0.01$ in benzene. The results are compiled in Table 5 together with rotational diffusion constants obtained from the relaxation data at 298 K.

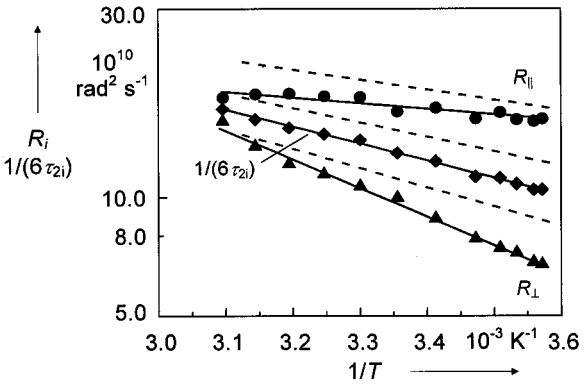

Figure 7. Rotational diffusion constants about the C_6 axis and perpendicular to it, $R_\|$ and $R_\perp$, respectively, and $1/(6\tau_i)$ from the NMR relaxation data. Lines represent the fit of an Arrhenius function to the NMR results (solid line) and to the MD simulation results for $1/(6\tau_{2\|})$, $1/(6\tau_{2\perp})$, and $1/(6\tau_{2i})$ (dashed line).

TABLE 5: Comparison of the Total Longitudinal ^{13}C Relaxation Rates $1/T_1$, Nuclear Overhauser Factors η_{C-H}, Dipolar Longitudinal Relaxation Rates $1/T_1^{DD}$, DD−CSA Cross Correlation Relaxation Rates $1/T_1^{DD-CSA}$, Rotational Diffusion Constants R_i, and $1/6\tau_i$ for Benzene in Neat Liquid and in a Polystyrene Solution with a Concentration of $x = 0.01$ (NMR) and 0.0093 (MD), Respectively

	neat liquid			polystyrene/ benzene (300 K)		
	NMR	MD (300 K)			MD	
	(298 K)	eq 31	eq 5	NMR	eq 31[a]	eq 5
$1/T_1/10^{-2}$ s^{-1}	3.61			18.6		
η_{C-H}	1.45			1.31		
$1/T_1^{DD}/10^{-2}$ s^{-1}	2.63			12.3		
$1/T_1^{DD-CSA}/10^{-2}$ s^{-1}	0.505			0.122		
$(1/6\tau_i)/10^{10}$ rad^2 s^{-1}	13.6	14		2.88	10	
$R_\perp/10^{10}$ rad^2 s^{-1}	9.42	11		0.241	1.3	
$R_\|/10^{10}$ rad^2 s^{-1}	19.1	17	17	<0!	<0!	9.2

[a] Data from refs 14, 15; considering $\tau_1 = 3\tau_2$ and $R_\perp = 1/(6\tau_\perp)$.

Discussion

Molecular Dynamics Simulations of Neat Benzene. From a least-squares fit to the data, the relation $\rho/(\text{kg m}^{-3}) = 1238 - 1.225\ T/\text{K}$ was obtained, whereas Klüner[41] found experimentally $\rho/(\text{kg m}^{-3}) = 1198 - 1.089\ T/\text{K}$. Thus, the thermal expansion coefficient from the MD simulations seems to be too large by about 12%.

The translational diffusion coefficient D for the benzene model used in the simulations is systematically too small by approximately a factor of 2 as has already been noted; the deviation between the experimental and MD results is a well-known deficiency of the chosen model.[14,15] A least-squares fit to the MD data between 280 and 360 K (refer to Figure 2) gives an activation energy of (15 ± 1) kJ/mol compared to an experimental value of 12.5 kJ/mol.[42] The slope becomes larger in the regime 240 to 280 K. Normally, such a break is taken as evidence for a change in the diffusion mechanism. It is noted here that the break occurs at the experimental melting point of benzene at 279 K. Although in the simulations neither freezing nor vitrification of the liquid was observed, it can be assumed that the system was in a supercooled state and that freezing was suppressed because of the form of the force field and/or the small system size. In order to prove that fact, the simulation at 240 K was extended to 1.1 ns without showing a slow-down of the diffusion process. Comparison with the experimental results for the temperature dependence of the translational diffusion coefficient should give some idea about the behavior

to be expected for reorientational motion: It appears that a deviation in the activation energy between MD and NMR results of about 2 kJ mol^{-1} is plausible. Furthermore, an increase of the activation energy below 280 K may be expected.

^{13}C Relaxation Data for Neat Benzene. As can be seen from Table 3 and Figure 3, the measured relaxation rates decrease with increasing temperature, which is the typical behavior in the extreme narrowing region, where $\omega\tau \ll 1$ is valid. The reorientational motion becomes faster with increasing temperature and the relaxation interactions less effective. From the reorientational parameters, the relaxation rates via the CSA relaxation mechanism were calculated with eq 35, and by subtracting them and the measured dipolar relaxation rates from the total relaxation rates, the rates from the spin rotation mechanism (SR) were obtained. The SR and CSA relaxation rates are also shown in Figure 3. The SR rates are the only rates that increase with increasing temperature and lead to a decrease in the absolute value of the slope for the total relaxation rate curve plotted as a function of $1/T$. Another way to obtain the CSA relaxation rates is to plot the total relaxation rates as a function of the square of the magnetic flux density (Figure 4). From the intercept with the relaxation rate axis, the sum over all relaxation rates contributing to the total rate except the CSA rate is yielded. In the present case, the value was $(3.47 \pm 0.03) \times 10^{-2}$ s^{-1}, which compares quite well with the value of 3.59×10^{-2} s^{-1} calculated from the reorientational parameters.

Rotational Molecular Dynamics of Neat Benzene. First, the MD results will be discussed. Figure 6 shows that $\tau_{1m,\mathrm{KWW}}$ is always larger than $\tau_{2m,\mathrm{KWW}}$: between 280 and 360 K, the correlation times for reorientations of in-plane vectors and vectors perpendicular to the aromatic plane are greater by factors of 2.5 and 3.0, respectively, whereas below 280 K, these ratios are different. For a given reorientation mode, the Debye model of small-step diffusion predicts the ratio τ_{2m}/τ_{1m} to have a value of 3.[19] The results show that this condition is fulfilled for reorientations about axes perpendicular to the C_6 axis. Another criterion of whether the investigated reorientational motions can be described by the Debye model is the value of the Kohlrausch exponent β_m^l: it is unity for small-step diffusion according to the Debye model. For all reorientational processes, the exponent approaches unity from below with increasing temperature. The exponent of reorientational motions of in-plane vectors reach the value of unity at lower temperatures (300 K) than the exponent of reorientations of vectors perpendicular to the plane (340 K). The fact that an exponent smaller than unity is predominately found at lower temperatures is in accordance with the assumption of supercooling, because $\beta_m^l < 1$ is often quoted to be a typical property for the dynamics of glassy systems.

The correlation times for reorientational motion of the C_6 axis is longer than for reorientations of vectors in the aromatic plane, and the activation energy is greater (cf. Table 4), whereas the activation energies are virtually identical for the same reorientational process but with different l. Hence, the activation energy differences between in-plane and tumbling motion are the same within the error limits, whether obtained for $l = 1$ (2.1 kJ mol^{-1}) or for $l = 2$ (2.3 kJ mol^{-1}). Below a temperature of 280 K, all activation energies become larger as in the case of translational diffusion, and also their differences increase (cf. Table 4). This indicates that, while both in-plane reorientations and reorientations of vectors perpendicular to the aromatic plane are slowed down by supercooling (cf. Figure 6), the latter are affected to a larger extent.

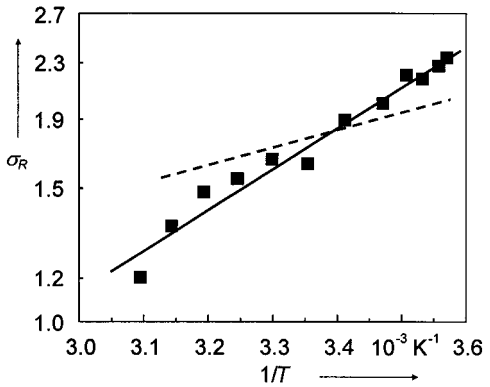

Figure 8. Anisotropy σ_R of the reorientational motion from the NMR relaxation data. Lines represent the fit of an Arrhenius function to the NMR results (solid line) and the fit of an Arrhenius function to the MD simulation results (dashed line).

As is demonstrated in Figure 7, the values for the velocity of reorientational motions obtained from the NMR experiments are generally smaller by 10 to 25% compared to the MD simulation results. Both methods agree, however, in that the rotation about the C_6 axis (spinning motion) is faster than about axes perpendicular to it (tumbling motion). The anisotropy $\sigma_R = R_{||}/R_\perp$ of reorientational motion is plotted in Figure 8 as a function of $1/T$. The anisotropy decreases with increasing temperature, and it follows an Arrhenius law to a very good approximation, for the simulation as well as for the NMR experiment. However, in the experiment, a slightly larger activation energy was obtained for the anisotropy. As a consequence, whereas the simulated and measured anisotropy show an excellent agreement to each other about room temperature, they diverge slightly at lower and higher temperatures. The value of approximately 1.7 for the anisotropy from the NMR experiments and the MD simulation at a temperature of about 300 K compares quite well with the more recent MD simulation results by Linse et al.[10] and Laaksonen et al.[18] (cf. Table 1). The recent experimental results all show a larger anisotropy between 2.4 and 2.9, except for the result by Dölle et al.[11] At a simulation temperature of 360 K, near the boiling point, the value from the MD simulation decreases to about 1.3 compared to the value of $\sqrt{1/2} \cong 0.71$ for the square root of the ratio of the corresponding correlation times for a free symmetric rotator. The NMR value for the activation energy $E_{A\perp}$ of 13.3 kJ mol^{-1} (cf. Table 4) is in good agreement with the value of 11.3 kJ mol^{-1} found by Patterson and Griffiths[43] from depolarized Rayleigh linewidths and also by Gillen and Griffiths[3] from Raman line shapes.

The χ test (eq 12) was applied to the rotational diffusion constants obtained from the NMR measurements: $\chi_\perp$ decreases from 6.6 to 3.1 for increasing temperature from 280 to 323 K, and $\chi_{||}$ decreases from 2.8 to 2.7. Thus, $\chi_{||}$ for rotational motions about the C_6 axis is not much greater than unity, and inertial effects are becoming important for these reorientational motions. According to the criterion by Gillen and Noggle,[34] the rotational motions about the C_6 axis are in the transitional range from inertially dominated reorientations to rotational diffusion ($3 < \chi < 5$), whereas the rotational motions about axes perpendicular to the C_6 axis change from the transitional range to the rotational diffusion range ($\chi < 5$) at about 293 K.

Solution of Polystyrene in Benzene. The total and dipolar relaxation rates for ^{13}C nuclei of benzene are greater than the rates for benzene in the neat liquid by one order of magnitude (Table 5). This indicates that the reorientational motion of vectors in the aromatic plane is slower than in the neat liquid

by approximately one quarter (cf. to the $1/(6\tau_{2i})$ in Table 5). The value of the cross correlation relaxation rate $1/T_1^{DD-CSA}$ is comparable to that for benzene in the neat liquid, and it should give, together with $1/(6\tau_{2i})$ the values for $R_\perp$ and $R_\parallel$.

For the apparent negative value of $R_\parallel$, which is obviously an artefact, several reasons are possible: The equations for the evaluation of the rotational dynamics from the relaxation rates are not applicable, because the reorientations of the benzene molecules are so slow that the extreme narrowing condition is not valid for the polystyrene/benzene solutions. This argumentation is not justified because the estimation of the extreme narrowing condition gives, even for the small value of $R_\perp$ a value much smaller than unity. Furthermore, measurements of spin−lattice relaxation rates at temperatures different from 300 K showed the temperature behavior expected for the extreme narrowing region. Equation 31 also yielded a negative value when applied to the MD simulation data.

However, from eq 31 it follows that for planar molecules that are symmetric rotators, $R_\parallel > 0$ is only true when the relation

$$\frac{1}{4}\frac{1}{6\tau_{2i}} \le R_\perp \le \frac{5}{2}\frac{1}{6\tau_{2i}} \quad (40)$$

holds. As is calculated from Table 5, this condition is not fulfilled for the benzene molecules in the solution of polystyrene in benzene. Thus, it can be concluded that the benzene molecules in the polystyrene solution do not reorient by a rotational diffusion process because reorientation about the C_6 axis is very much faster than about axes in the aromatic plane. The benzene molecules reorient about the C_6 axis in their own volume, whereas for rotations about axes perpendicular to it, the surrounding cavity built out of the polymer has to be deformed substantially, a process that is hindered by a much higher activation barrier. This argument is supported by the results of Müller-Plathe,[14,15] who studied the polystyrene/benzene system by MD simulations and concluded that for an increasing polystyrene concentration, a drastic slowing-down of reorientations about axes in the aromatic plane occurred, whereas rotations about the normal of the aromatic plane were only moderately affected. A similar observation, although smaller in magnitude, was made for water mixtures with poly(vinyl alcohol):[16] The reorientation of the dipole vector slows down much more with increasing polymer content than the reorientations about the other two principal axes.

The authors believe that the apparent negative values of $R_\parallel$ deduced from $R_\perp$ and $1/(6\tau_{2i})$ arise because the reorientational motions of the benzene molecules in the polystyrene matrix show a very large anisotropy. Yet, the benzene molecules exhibit a "one−dimensional rotational diffusion" about the C_6 axis, whose orientation is practically fixed. To prove this concept, additional short simulations of a few picoseconds for neat benzene as well as for the benzene/polystyrene system were performed under conditions identical to those in refs 14 and 15. However, the trajectories were recorded much more frequently than before, that is, every 10 fs. Thus, the angular velocity autocorrelation function $\langle\omega_\parallel(t)\omega_\parallel(0)\rangle$ for reorientations about the C_6 axis could be calculated directly with sufficient resolution. It turns out that the qualitative features are the same for both neat benzene and benzene in polystyrene: After removing a spurious vibrational component by low-pass filtering, the normalized correlation function was well fitted by the sum of a Gaussian and an exponential function,

$$\langle\omega_\parallel(t)\omega_\parallel(0)\rangle \cong A\exp[-(t/B)^2] + (1-A)\exp(-t/C) \quad (41)$$

In both cases, the Gaussian, being characteristic for short-time inertial rotational motions, contributes about three quarters to the correlation functions. Its time constant B is very similar for neat benzene (0.165 ps) and benzene in polystyrene (0.174 ps). This means that the inertial rotational motion shows very little sensitivity to the environment. The exponential term corresponds to long-term Debye-like rotational diffusion, albeit in one dimension only. Its characteristic time differs by a factor of about 2 for neat benzene (0.457 ps) and benzene in polystyrene (0.231 ps). The time integral of the correlation function from eq 41 yields (cf. eq 5) the rotational diffusion coefficients $R_\parallel$. Since the integral is dominated by the Gaussian contribution, the raw $R_\parallel$ are quite similar for neat benzene (33×10^{10} rad^2 s^{-1}) and benzene in PS (26×10^{10} rad^2 s^{-1}). The short-time Gaussian behavior, however, manifests itself in the NMR experiment and the alternative MD analysis via the reorientation of unit vectors only as an offset (cf. eq 10 and 22), because both are much more sensitive to the long-time behavior. For a comparison, it is therefore better to concentrate on the exponential part only. Its integrals lead to the second set of $R_\parallel$ in Table 5. The consistency between the two ways of calculating $R_\parallel$ is seen in the MD value for neat benzene, which is identical for both sets. The presence of polystyrene slows down the parallel reorientation of benzene by a factor of about 1.8. However, this value is still of the same order as in neat benzene, so the very small or even negative values predicted by the rotational diffusion model are obviously an artefact. This, of course, also applies to the $R_\parallel$ determined from the NMR relaxation data. A nice corroboration of the hypothesis of "one−dimensional rotational diffusion" is provided by the agreement of $1/(6\tau_{2i})$ and $R_\parallel$. They can only be the same if the rotation about the C_6 axis is as fast as the rotation of an in-plane vector, that is, if the reorientations about axes perpendicular to the C_6 axis can be neglected.

When the results in Table 5 are taken to estimate the effect of the polystyrene, although the reorientational motions of the benzene molecules do not seem to occur by a three-dimensional rotational diffusion process, the experimentally found differences between the solution and neat liquid appear to be much more pronounced than when compared to the results from the MD simulations (cf. Table 5). In analogy to our results, Lienin et al.[44] were also not able to describe the rotational motion of small molecules in a oligomer matrix by simple rotational diffusion models. Another report of benzene reorientation in a oligostysrene matrix was given by Vogel and Rössler,[45] who, however, did not investigate the anisotropy of the reorientational motions.

Conclusions

A good agreement between the NMR and MD simulation results for the reorientational motions of benzene in the neat liquid as well as in a polystyrene/benzene solutions was obtained in this study. Although the reorientational motions of benzene are significantly anisotropic, the results show a more isotropic reorientational motion for benzene in the neat liquid than in most other studies. The anisotropy decreases with temperature, which is explained by the concept that tumbling of the molecule needs more space than mere spinning, and thus, the difference in the rotational velocities should be more pronounced at higher densities. The activation parameters for the rotations about the C_6 axis and perpendicular to it are, to the authors knowledge, available now for the first time. Whereas the MD data showed that the reorientational correlation functions do not decay exponentially, it can be concluded that for the reorientational

process about the C_6 axis, inertial effects already become important. The measurement of the DD−CSA cross correlation rates proved to be a valuable tool in the investigation of rotational motions of aromatic molecules.

The present investigation of the rotational motions of benzene molecules in a polystyrene matrix demonstrates that the Debye model of independent rotational diffusion about the three molecular axes is not valid for describing the reorientational motions of small molecules in restricted geometries like polymer matrices. Here, the detailed analysis of the MD results for the benzene/polystyrene system shows that the C_6 axis becomes space-fixed and that rotational diffusion is only possible about this axis. This reduces the number of rotational degrees of freedom in a first approximation from three to one. Rotational diffusion constants calculated from the MD simulations are consistent with this picture, whereas rotational diffusion constants inferred from a model of three-dimensional rotational diffusion have no obvious physical meaning. More generally, the Debye model for rotational diffusion should be applied only with extreme care when the reorientation of molecules in restricted geometries is investigated.

Methods

MD Simulations. The OPLS model for liquid benzene[46] was applied. Since the MD simulation program[47] used does not handle completely rigid molecules, the OPLS model was extended by harmonic angle bending and torsional terms. This model was used previously to study polystyrene/benzene mixtures[14,15] and is described in detail in ref 15. The simulated system consisted of 215 benzene molecules under cubic periodic boundary conditions. Temperature and pressure were kept constant using the method of Berendsen[48] with coupling times of 0.2 ps for the temperature and 0.5 ps for the pressure. The reference pressure was 0.1013 MPa; the temperatures investigated are given in Table 2. The time step was 2 fs, and the durations of the simulations are also shown in Table 2. The bond lengths were constrained by the SHAKE procedure with a relative tolerance of 10^{-6}.

The translational diffusion coefficients were calculated from the center-of-mass mean−square fluctuation, averaged over all molecules as well as over the time origins (cf. ref 15); the standard deviation among the three Cartesian components was taken as an error estimate.[49,50]

For the study of the reorientational dynamics of benzene, two vectors for each molecule were defined: $\boldsymbol{u}_i$ as the unit vector between two opposite carbons—because of the symmetry of the benzene molecule, all in-plane vectors are equivalent—and $\boldsymbol{u}_n$ as the normal on the aromatic plane. The time evolution of the orientation is described by time autocorrelation functions $C_0^l(t)$ with $l = 1, 2$ in eqs 18 and 19 for these vectors. Fitting of the correlation functions to the Kohlrausch−Williams−Watts function in eq 13 and computing their integrals by eq 14 yielded the correlation times $\tau_{l\parallel}$ and $\tau_{l\perp}$.

^{13}C NMR Relaxation Data. The measurements were performed on a Bruker AM 250 spectrometer ($B_0 = 5.875$ T, $\nu_0(^1\mathrm{H}) = 250.13$ MHz, $\nu_0(^{13}\mathrm{C}) = 62.90$ MHz, lock on ^{2}H in [$^2H_6$]acetone in a 10-mm NMR tube surrounding the inner NMR tube with 7.5-mm diameter containing benzene or the polystyrene/benzene solution). For the experimental parameters of the ^{13}C measurements at 75.47 and 100.62 MHz cf. to refs 11 and 51. Measurements of the spin−lattice relaxation times were carried out using the inversion-recovery pulse sequence, varying in 20 experiments the delays between the pulses in a range from 0.1 s to 0.6 T_1 and 0.8 to 1.5 T_1, whereas the fully relaxed spectrum was observed three times at 5 T_1. The spin−lattice relaxation times were extracted from the signal heights in the ^{1}H broadband decoupled ^{13}C spectra by a three-parameter exponential fit implemented in the spectrometer software. The dipolar relaxation rates were obtained from the relation

$$\frac{1}{T_1^{\mathrm{DD}}} = \frac{\eta_{\mathrm{C-H}}}{\eta_{\mathrm{C-H,max}}}\frac{1}{T_1} \tag{42}$$

with $\eta_{\mathrm{C-H,max}} = 1.988$ as the maximum nuclear Overhauser factor.

The application of the inversion−recovery sequence on a ^{1}H−^{13}C spin system without decoupling of the protons yields a spectrum that has approximately the appearance of a doublet and that shows different signal heights as a function of the delay between the first and the second pulse. The sum and the difference of the two signal heights correspond to magnetization modes ν_1 and ν_3, respectively. In the initial slope approximation, all contributions to the slope of mode ν_3 except the contribution resulting from the DD−CSA cross correlation vanish:

$$\lim_{t\to 0} \dot{\nu}_3(t) = 2\Gamma_{13} I_{\mathrm{C}}^{\mathrm{eq}} \tag{43}$$

Thus, the obtained FIDs were treated with an exponential multiplication and an artificial line-broadening factor of 6 Hz in order to smear out the long-range ^{13}C−^{1}H couplings. This procedure allows treatment of the ^{13}C−^{1}H coupled spectrum in a first-order approximation as an AX spectrum. Then, the differences of the line heights were taken, and the slope was determined numerically by fitting a linear function or a second-order polynomial to the experimental data from 10 experiments with different delays between the pulses. To show the difference between the linear and the polynomial fit, the results for the initial slopes are compared in Figure 9 for 298 K. For a linear fit of the data with $t \le 4$ s, the linear equation is $\nu_3/I_{\mathrm{C}}^{\mathrm{eq}} = 1.19 \times 10^{-3} + 9.08 \times 10^{-3}\, t/\mathrm{s}$, whereas it is equal to $2.86 \times 10^{-3} + 7.34 \times 10^{-3}\, t/\mathrm{s}$ for $t \le 7$ s. When employing a polynomial fit of second order, the equations are $\nu_3/I_{\mathrm{C}}^{\mathrm{eq}} = 8.39 \times 10^{-4} + 0.996 \times 10^{-2}\, t/\mathrm{s} - 2.28 \times 10^{-4}\, t^2/\mathrm{s}^2$ and $5.70 \times 10^{-4} + 1.09 \times 10^{-2}\, t/\mathrm{s} - 5.52 \times 10^{-4}\, t^2/\mathrm{s}^2$, respectively. The difference in the slope for the linear terms is about 9% for the polynomial and more than double for the linear fit. The example shown is one of the worse cases; normally, the difference between the slopes was much smaller for the polynomial fit. Furthermore, the data were restricted to $t \le 4$ s, for which case the differences became negligible. These results show clearly the superiority of the polynomial over the linear fit for evaluating initial slopes of the DD−CSA cross correlation rate, because the ambiguity regarding the selection of the time interval for which the initial slope approximation is fulfilled is strongly diminished.

The measurements of the spin−lattice relaxation times were repeated 5 times, those for the NOE factors 10 times, and those for the DD−CSA cross correlation relaxation rates 5 times. The mean standard deviations of the mean experimental data were below 1% for the dipolar spin−lattice relaxation times and less than 2.5% for the cross correlation relaxation rates. The error in the temperature was estimated to be ±1 K. Further details concerning experimental techniques and sample preparation are given in ref 52.

For the evaluation of the rotational dynamics, a distance between the carbon atom and the directly bonded proton of 110.6 pm was used, which was the effective distance obtained from vibrational averaging for the dipolar coupling constant.[53] The protons not directly bonded were taken into account by summing

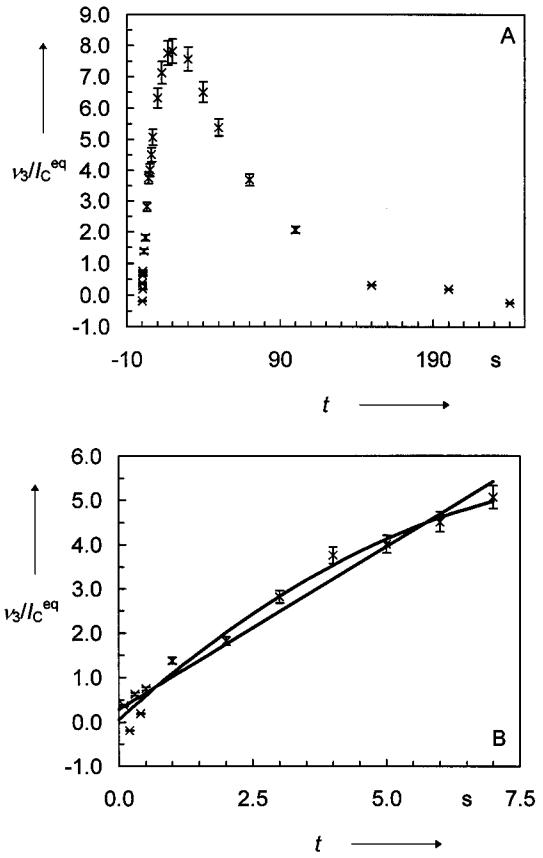

Figure 9. Magnetization mode ν_3 as a function of time (A) and linear and polynomial fit of second order to the initial slope (lines) (B). The error bars correspond to an error of 5%.

up their contributions to the dipolar coupling constant,[11] and thus the total effective distance was 109.7 pm. The rotational diffusion constants were calculated by solving eqs 29 and 38, using also eq 25 for $R_{||}$ and $R_{\perp}$. The values for $\Delta\sigma$ and η were taken from the literature to be 182 ppm and 0.72, respectively.[54] The computation of the activation parameters for the reorientational motion was achieved by a FORTRAN 77 program, which performed a χ^2 fit of the activation parameters to the experimental reorientational data by the Levenberg−Marquardt method.[55]

Acknowledgment. Financial support by the Fonds der Chemischen Industrie is gratefully acknowledged. The authors thank M.D. Zeidler for helpful discussions and his support of this work, P. Mutzenhardt for his comments, and P. Blümler for his help.

References and Notes

(1) Huntress, W. T. *J. Phys. Chem*. **1969**, *73*, 103.
(2) Bartoli, F. J.; Litovitz, T. A. *J. Chem. Phys*. **1972**, *56*, 413.
(3) Gillen, K. T.; Griffiths, J. E. *Chem. Phys. Lett*. **1972**, *17*, 359.
(4) Bauer, D. R.; Alms, G. R.; Brauman, J. I.; Pecora, R. *J. Chem. Phys*. **1974**, *61*, 2255.
(5) Tanabe, K.; Jonas, J. *J. Chem. Phys*. **1977**, *67*, 4222.
(6) Yamamoto, O.; Yanagisawa, M. *Chem. Phys. Lett*. **1978**, *54*, 164.
(7) Tanabe, K. *Chem. Phys. Lett*. **1979**, *63*, 43.
(8) Tanabe, K.; Hiraishi, J. *Mol. Phys*. **1980**, *39*, 493.
(9) Steinhauser, O. *Chem. Phys*. **1982**, *73*, 155.
(10) Linse, P.; Engström, S.; Jönsson, B. *Chem. Phys. Lett*. **1985**, *115*, 95.
(11) Dölle, A.; Suhm, M. A.; Weingärtner, H. *J. Chem. Phys*. **1991**, *94*, 3361.
(12) Coupry, C.; Chenon, M.-T.; Werbelow, L. G. *J. Chem. Phys*. **1994**, *101*, 899.
(13) Yi, J.; Jonas, J. *J. Phys. Chem*. **1996**, *100*, 16789.
(14) Müller-Plathe, F. *Chem. Phys. Lett*. **1996**, *252*, 419.
(15) Müller-Plathe, F. *Macromolecules* **1996**, *29*, 4782.
(16) Müller-Plathe, F. *J. Chem. Phys*. **1998**, *108*, 8252; *Macromolecules* **1998**, *31*, 6721; *Ber. Bunsen-Ges. Phys. Chem*. **1998**, *102*, 1679.
(17) Python, H.; Mutzenhardt, P.; Canet, D. *J. Phys. Chem. A* **1997**, *101*, 1793.
(18) Laaksonen, A.; Stilbs, P.; Wasylishen, R. *J. Chem. Phys*. **1998**, *108*, 455.
(19) McQuarrie, D. A. *Statistical Mechanics*; Harper & Row: New York, 1973.
(20) Allen, M. P.; Tildesley, D. J. *Computer Simulation of Liquids*; Oxford University Press: Oxford, 1991.
(21) Steele, W. A. *J. Chem. Phys*. **1963**, *38*, 2404.
(22) Huntress, W. T. *Adv. Magn. Reson*. **1970**, *4*, 1.
(23) Woessner, D. E. *J. Chem. Phys*. **1962**, *37*, 647.
(24) Favro, D. L. *Phys. Rev*. **1960**, *119*, 53.
(25) Huntress, W. T. *J. Chem. Phys*. **1968**, *48*, 3524.
(26) Steele, W. A. *J. Mol. Liq*. **1984**, *29*, 209.
(27) Grant, D. M.; Brown, R. A. Relaxation of Coupled Spins from Rotational Diffusion. In *Encyclopedia of Nuclear Magnetic Resonance*; Grant, D. M., Harris, R. K., Eds.; John Wiley & Sons: New York, 1995.
(28) Steele, W. A. *J. Chem. Phys*. **1963**, *38*, 2411.
(29) Steele, W. A. *Adv. Chem. Phys*. **1976**, *34*, 1.
(30) Valiev, K. A.; Ivanov, E. N. *Sov. Phys.-Usp*. **1973**, *16*, 1.
(31) Dölle, A.; Bluhm, T. *Progr. Nucl. Magn. Reson. Spectrosc*. **1989**, *21*, 175.
(32) Beckmann, P. A. *Phys. Rep*. **1988**, *171*, 85.
(33) Wallach, D.; Huntress, W. T. *J. Chem. Phys*. **1969**, *50*, 1219.
(34) Gillen, K. T.; Noggle, J. H. *J. Chem. Phys*. **1970**, *53*, 801.
(35) Kohlrausch, F. *Pogg. Ann*. **1863**, *119*, 337.
(36) Williams, G.; Watts, D. C. *Trans. Faraday Soc*. **1970**, *66*, 80.
(37) Lindsey, C. P.; Patterson, G. D. *J. Chem. Phys*. **1980**, *73*, 3348.
(38) Bloembergen, N.; Purcell, E. M.; Pound, R. V. *Phys. Rev*. **1948**, *73*, 679.
(39) Canet, D. *Progr. Nucl. Magn. Reson. Spectrosc*. **1989**, *21*, 237.
(40) Neuhaus, D.; Williamson, M. *The Nuclear Overhauser Effect in Structural and Conformational Analysis*; VCH Publishers: New York, 1989.
(41) Klüner, R. P. *Rotatorische Dynamik von Kohlenwasserstoffen in flüssiger Phase*; Shaker-Verlag: Aachen, 1995.
(42) Ertl, H.; Dullien, F. A. L. *AIChE J*. **1973**, *19*, 1215.
(43) Patterson, G. D.; Griffiths, J. E. *J. Chem. Phys*. **1975**, *63*, 2406.
(44) Lienin, S. F.; Brüschweiler, R.; Ernst, R. R. *J. Magn. Reson*. **1998**, *131*, 184.
(45) Vogel, M.; Rössler, E. *J. Phys. Chem. A* **1998**, *102*, 2103.
(46) Jorgensen, W. L.; Severance, D. L. *J. Am. Chem. Soc*. **1990**, *112*, 4768.
(47) Müller-Plathe, F. *Comput. Phys. Commun*. **1993**, *78*, 77.
(48) Berendsen, H. J. C.; Postma, J. P. M.; van Gunsteren, W. F.; Di Nola, A.; Haak, J. R. *J. Chem. Phys*. **1984**, *81*, 3684.
(49) Müller-Plathe, F. *Mol. Sim*. **1996**, *18*, 133.
(50) Müller-Plathe, F.; van Gunsteren, W. F. *Polymer* **1997**, *38*, 2259.
(51) Gruhlke, P.; Dölle, A. *J. Chem. Soc., Perkin Trans. 2* **1998**, 2159.
(52) Dölle, A.; Bluhm, T. *J. Chem. Soc., Perkin Trans. 2* **1985**, 1785.
(53) Hardy, E. H.; Witt, R.; Dölle, A.; Zeidler, M. D. *J. Magn. Reson*. **1998**, *134*, 300.
(54) Strub, H.; Beeler, A. J.; Grant, D. M.; Michl, J.; Cutts, P. W.; Zilm, K. W. *J. Am. Chem. Soc*. **1983**, *105*, 3333.
(55) Press, W. H.; Flannery, B. P.; Teukolsky, S. A.; Vetterling, W. T. *Numerical Recipes. The Art of Scientific Computing*; Cambridge University Press: Cambridge, 1989.